NATIONAL BUREAU OF STANDARDS

Technical News

BULLETIN

VOLUME 49

NUMBER 1

JANUARY 1965

NATIONAL BUREAU OF STANDARDS

Technical News

B U L L E T I N

January 1965 **Issued Monthly** **Vol. 49, No. 1**

Cover design was suggested by changing patterns on the oscilloscope screen used to detect unbalance of bridge circuit for calibrating inductive voltage dividers. The drawing (left) gives a more realistic rendering of successive appearances of the screen as balance is approached. Several stages in the process are shown simultaneously; lines become heavier as balance is approached. (For further details, see p. 2.)

Electrical Calibration Service Extended

inductive voltage dividers calibrated up to 10 kHz

The Washington laboratories of the Bureau now provide a service for the precise calibration of inductive voltage dividers at frequencies up to 10 kHz.[1] Similar calibrations at 100, 400, and 1000 Hz have been available for some time.[2]

In the last 10 years or so, the accurate measurement of voltage-ratio and phase-angle has become of critical importance in a number of areas of pure and applied research. It is also the key operation, for example, in many missile component production processes. Inductive voltage dividers have been a natural choice for such determinations because of the high accuracy of which they are capable. It is therefore a continuing responsibility of the national laboratories to improve their capabilities in the techniques of voltage ratio measurement, and to maintain the highest possible level of accuracy in these measurements.[3,4]

The new calibration service, which constitutes a significant extension of the Bureau's basic electrical measurements program, insures a uniform basis for voltage ratio measurements in this country.

Calibration accuracy for a first-quality divider operating at its optimum designed frequency is normally stated to be within 0.5 part per million of the input for frequencies up to 2 kHz; and it decreases progressively with increasing frequency, falling to 5 parts per million of the input at 10 kHz.

Inductive voltage dividers consist in general of five to seven autotransformer-type windings, multi-tapped, on tape-wound toroidal cores of very high magnetic permeability. All windings are connected in a modified Kelvin-Varley slide arrangement.

Comparison Method

For frequencies up to about 2 kHz, a comparison method providing a simple and efficient calibration service without excessive degradation of accuracy is used. The method was initially developed by Wilbur Sze. It was further investigated and some modifications were made by T. L. Zapf and R. V. Lisle for the setup used at the NBS Boulder laboratories.[5]

The circuit (*diagram p. 3*) requires little equipment other than a "standard" seven-decade inductive voltage divider (i.e., one that has been calibrated directly in terms of an impedence divider) of very small phase-angle error. Because of the small phase-angle error requirement, it is necessary to use several calibrated dividers to cover the entire frequency range up to 10 kHz. At present two "standard" voltage dividers are being used in Washington, one for measurements up to about 100 Hz, the other for measurements to about 2 kHz. A third divider is being calibrated for measurements from 3 to 10 kHz.

A capacitance-resistance network, located as shown in the diagram, produces a component of voltage which is in quadrature with the supply voltage. At balance, this quadrature voltage is equal, but in opposing polarity, to that resulting from the small phase-angle difference between the output voltages of the "standard" and the "test" dividers, and this phase difference is approximately equal to $-2\pi fCR$ radians (the ratio of R to the capacitive reactance).

The in-phase voltage balance is achieved by adjusting the lower dials of the "standard" divider.

A "guard" inductive voltage divider serves to eliminate stray capacitive current between the detector circuit and its shield. This is accomplished by setting the output tap of the "guard" divider equal to that of the "test" divider.

Capacitance Divider Method

For the present, in the range from 3 to 10 kHz, inductive voltage dividers are calibrated by direct comparison with a capacitance divider made up of three-terminal capacitors whose relative values are obtained by intercomparison in a bridge having transformer-type ratio arms.[6]

With the "test" divider input connected across one arm of the bridge circuit (*see illustration*), balance is
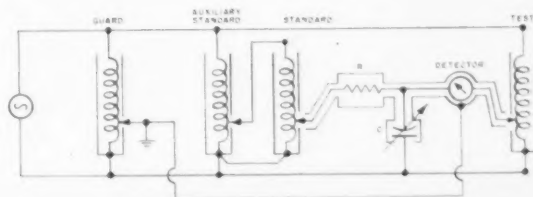
Comparison circuit, modified for calibrating the lower decades.

achieved by adjusting the output taps, N_1 and N_2, of two other inductive voltage dividers which are connected across the 0.1-V taps of the ratio-arm transformer. $\overset{N}{\underset{1}{\Sigma}} C_2$ consists of an appropriate number, N, of capacitors of the same nominal values. N depends on the setting of the dials on the "test" divider. C_1 is larger than C_2 by a factor of 10 or more depending on the ratio of the "test" divider.

The in-phase voltage balance is achieved by insertion of a current into the detector junction of the bridge through capacitor C_5. The phase differences between the bridge arms are compensated for by insertion of a quadrature current of appropriate magnitude into the detector junction of the bridge through resistor R and current divider $C_3/(C_3+C_4)$. These techniques have been fully described by McGregor et al.[7]

The "test" divider is then disconnected from the bridge and the individual units, C_2, making up $\overset{N}{\underset{1}{\Sigma}} C_2$ are compared with C_1. The capacitance divider ratio is thus determined to a great accuracy by a substitution method in which the exact values of C_1 and C_2 need not be known. However, these must be very stable capacitors of negligibly small voltage coefficient. As in the previous arrangement, the in-phase and quadrature differences between the bridge arms are compensated for by insertion of currents of appropriate phase and magnitude.

The voltage-ratio and phase-angle errors of the "test" divider can then be determined from the differences of the N_1 and N_2 settings for the two balances.

Split-Sweep Detector

This oscilloscope presentation (*see drawing, inside front cover*) is used with the capacitance divider method.

Balance in both in-phase and quadrature components is attained more or less simultaneously by adjusting two controls. Approach to balance in quadrature makes the minor axes of the two ellipses shrink, and at quadrature balance the ellipses become straight segments. If the segments (or, more generally, the major axes of the ellipses) are not in the same straight line, there is unbalance in the in-phase component. Complete balance is indicated by a pattern of two segments that lie in a straight line.

The double pattern, simulating a double-beam oscilloscope, is traced starting from the center of screen. This is achieved by superimposing a square wave on the hozizontal sweep voltage, which makes each sweep begin at the center, move to right, fly back to far left, and finally move right to center where sweep ends. Start and finish of the sweep are thus brought into juxtaposition, and their coincidence (or lack of it) is a positive and sensitive indicator of balance (or lack of it).

Chiefly responsible for this "split sweep" technique are W. K. Clothier of the National Standards Laboratory, Australia, and R. C. Cutkosky of NBS.

Calibration of the Lower Decades

The calibration service includes determination of the voltage-ratio and phase-angle errors of the inductive voltage divider for each setting of each of the three highest decades (all decades except the one under calibration being set at zero). This calibration is believed adequate for most measurement purposes.

If calibration of the lower decades should be necessary, a simple and effective modification of the comparison circuit can be made. This is done (*see diagram, p. 1*) by adding an "auxiliary standard" divider whose three highest decades have been calibrated either by the Bureau or by the user. The input of the "standard" divider should be connected to the output of the "auxiliary standard" divider; and the input circuits of the "auxiliary standard" and "test" dividers should be paralleled and the phase-balancing and detector networks connected as when performing a comparison calibration.

Care should be taken to insure that the load imposed on the "auxiliary standard" by the "standard" divider is not so large that it causes a significant error in the measurements. This loading error can be minimized by having the "auxiliary standard" set at the lowest calibrated setting.

For example, if the test divider is set at 0.0001, balance will be obtained with the "standard" set at 0.1 and the "auxiliary standard" set at 0.001 (the lowest calibrated setting). The fourth decade of the "test" divider may then be calibrated to 6 or 7 significant figures. Such a method would be satisfactory for the calibration of the lower decades in the user's own laboratory.

[1] *The new service is offered by the High-Voltage Section, Electricity Division, National Bureau of Standards, Washington, D.C. 20234.*

[2] *In particular, calibrations of the same high accuracy at 400 and 1000 Hz are and have been available also from the NBS Boulder Laboratories. The present article, except for incidental references to Boulder, deals exclusively with services of the Washington Laboratories. Inquiries concerning the calibration services at Boulder should be addressed to: Low-Frequency Calibration Services, Radio Standards Engineering Division, National Bureau of Standards, Boulder, Colo. 80301.*

[3] Measurement of voltage ratios at audio frequencies, by *Wilbur C. Sze, Trans. AIEE, Pt. I,* **76**, 444 (1957).

[4] A seven-decade adjustable-ratio inductive-coupled voltage divider with 0.1 part per million accuracy, by *J. J. Hill and A. P. Miller, JIEE* **109B**, 157–162 (1962).

[5] Comparison calibration of inductive voltage dividers, by *R. V. Lisle and T. L. Zapf, ISA Trans.* **3**, 228–232 (1964).

[6] The precision measurement of transformer ratios, by *R. D. Cutkosky and J. Q. Shields, IRE Trans. Instr.* **I–9**, 243 (1960).

[7] New apparatus at the NBS for absolute capacitance measurement, by *M. C. McGregor, J. F. Hersh, R. D. Cutkosky, F. K. Harris, and F. R. Kotter, IRE Trans. Instr.* **I–7**, 253 (1956).

DETECTOR

TEST DIVIDER

BRIDGE TRANSFORMERS
HIGH f   LOW f   HIGH f

$\sum_{1}^{N} C_2$

C_5

C_3, C_4
& R

N_1

N_2

C_1

BRIDGE RATIO ARM
TRANSFORMER

TEST DIVIDER

DETECTOR C_5 C_1

N_1

N_2

C_4

C_3 $\sum_{1}^{N} C_2$

R
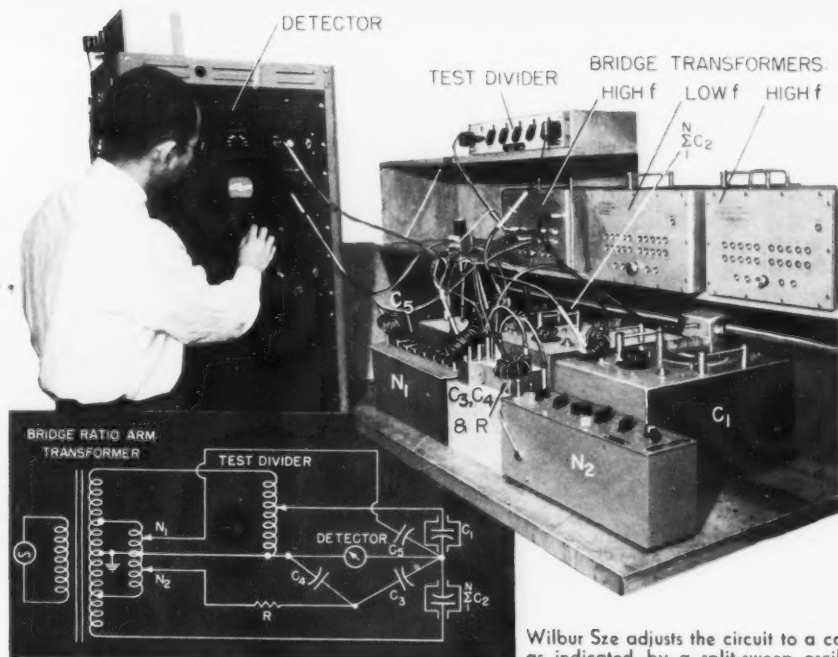
Wilbur Sze adjusts the circuit to a condition of "balance" as indicated by a split-sweep oscilloscope presentation. Balance is attained when the two ellipses flatten into segments that lie along the same straight line. Shielding is not shown in detail in the circuit diagram.

POWER
SUPPLY   C   GUARD DIVIDER   STANDARD DIVIDER

R

TEST DIVIDER

DETECTOR

GUARD   STANDARD   R   DETECTOR   TEST

C

Circuit for calibration of inductive voltage dividers by comparison with a "standard" divider.
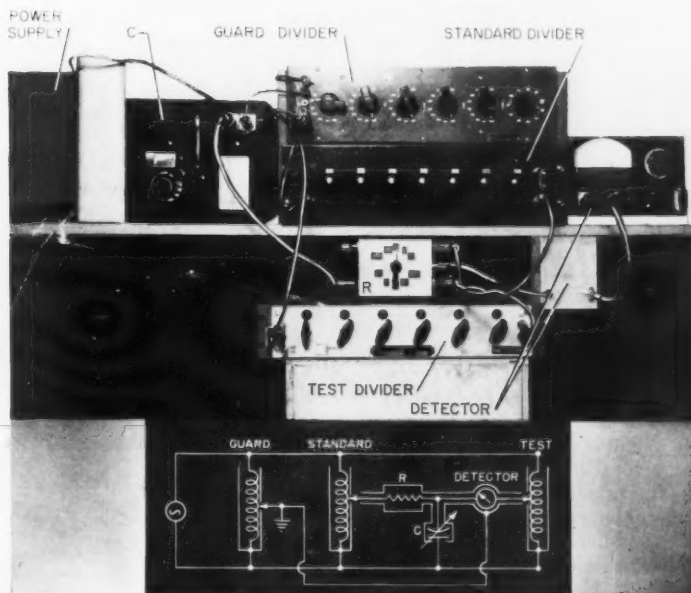
Portable Atomic Frequency Standard
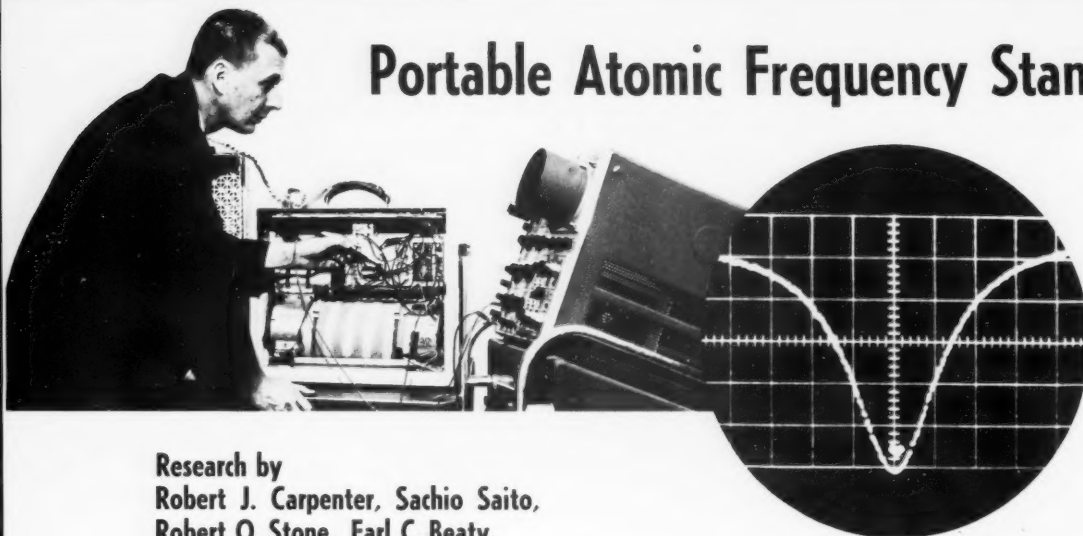
Research by
Robert J. Carpenter, Sachio Saito,
Robert O. Stone, Earl C. Beaty,
and Peter L. Bender

Left: Robert Carpenter inspects waveform obtained from a portable rubidium vapor frequency standard. (Photo courtesy of NASA.) *Right:* Response of rubidium cell as frequency is swept across atomic transition reference; each large horizontal division is approximately 20 Hz.

A rubidium-vapor frequency standard developed at NBS for NASA combines the accuracy and stability of atomic standards with easy portability and independence of power lines.[1] The standard has a short-term stability better than 1 part in 10^{10}, recommending it for use both as a clock and as a frequency standard. Lightweight and requiring approximately 23 W of power, it is useful for synchronizing clocks in isolated areas to which it can be transported. Normally it operates from conventional a-c power; if power is removed it switches automatically to self-contained batteries for approximately 8 hr of operation at room temperature.

Transition Method Used

Atomic frequency standards operate by one of two means: by determining the frequency corresponding to dipole inversion in a beam of atoms, or by determining the frequency corresponding to a transition between the energy levels of atoms in a fixed sample. The transition method[2] is used in the rubidium frequency standard; rubidium vapor in a cell is stimulated by a beam of light, causing two kinds of energy transitions to occur in the cell.

The stimulating light is scattered most when the populations of the two different ground states are equal. Conversely, more stimulating light passes straight through the cell when the population difference is greatest, producing maximum response of a photoelectric cell placed in the path of the emerging beam. The operation of the rubidium standard uses the fact that the transmitted light intensity is decreased in the presence of a magnetic field oscillating at a frequency known as the rubidium hyperfine frequency. The samples in the rubidium standards have been selected so that population difference is low, and photocell indication least, when a microwave field at a frequency of 6 834 683 405 Hz is applied to the cell.

Like most atomic clocks, the rubidium clock operates in an indirect way to sense the frequency of the atomic reference. The applied microwave field is frequency-modulated at an audio rate, the frequency of the atomic transition is sensed, and the average frequency of the field is modified by servo circuits to center the transition frequency in the sweep. The sweep center frequency is then the transition frequency sought.
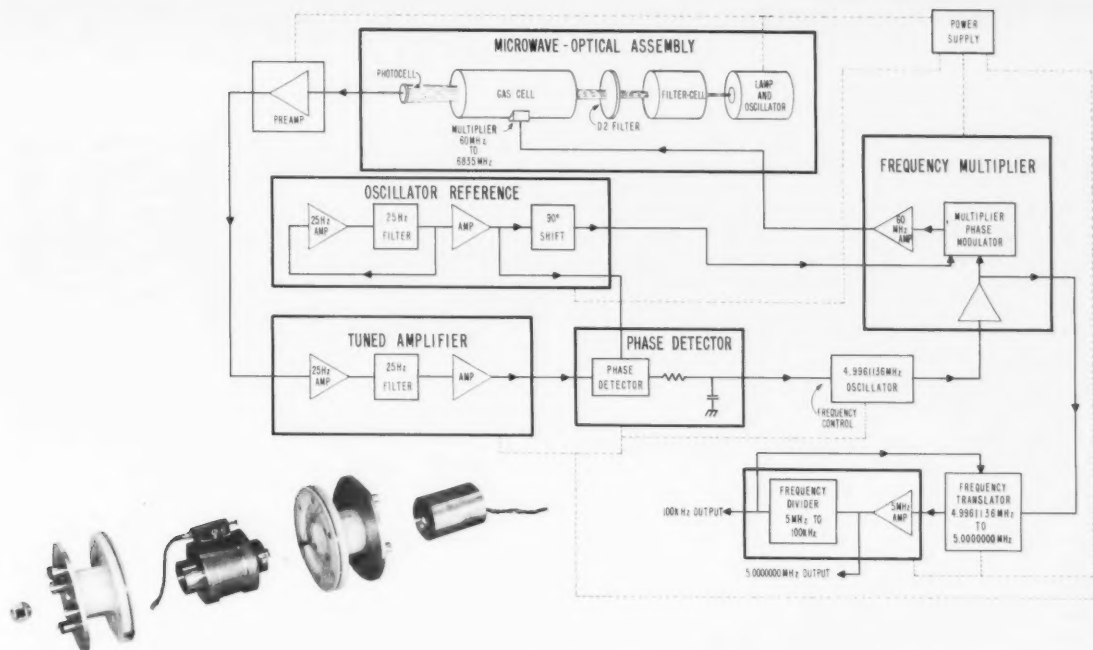
Operation of the Standard

Since the rubidium frequency standard weighs only 18 kg (39 lb) and its power supply 26 kg, it is easily transportable. It will operate on battery power for at least 5 hr, and up to 15 hr if the ambient temperature is near 45° C and minimum power is required to maintain the device's temperature. The batteries are recharged and maintained in fully charged condition during line-power operation.

The portability of this frequency standard and its ability to operate without line power make it ideal for time comparisons at isolated facilities. It makes possible the comparison of geographically separated clocks without errors or phase ambiguities due to variations in radio propagation paths.

[1] *For details, see* A portable rubidium-vapor frequency standard, *by Robert J. Carpenter, NBS Tech. Note 235 (Apr. 1964); also,* A prototype rubidium vapor frequency standard, *by R. J. Carpenter, E. C. Beaty, P. L. Bender, S. Saito, and R. O. Stone, IRE Trans. Instr.* I–9, *132–135 (Sept. 1960).*

[2] Optical detection of narrow Rb₈₇ hyperfine absorption lines, *by P. L. Bender, E. C. Beaty, and A. R. Chi, Phys. Rev. Letters* 1, *311–313 (Nov. 1958).*

POWER SUPPLY

MICROWAVE - OPTICAL ASSEMBLY

PHOTOCELL
GAS CELL
LAMP AND OSCILLATOR
D2 FILTER
FILTER-CELL
MULTIPLIER 60 MHz TO 6835 MHz
PREAMP

FREQUENCY MULTIPLIER
60 MHz AMP
MULTIPLIER PHASE MODULATOR

OSCILLATOR REFERENCE
25 Hz AMP
25 Hz FILTER
AMP
90° SHIFT

TUNED AMPLIFIER
25 Hz AMP
25 Hz FILTER
AMP

PHASE DETECTOR
PHASE DETECTOR

4.996I|36 MHz OSCILLATOR
FREQUENCY CONTROL

FREQUENCY DIVIDER 5 MHz TO 100 kHz
100 kHz OUTPUT
5 MHz AMP
FREQUENCY TRANSLATOR 4.996I136 MHz TO 5.000000 MHz
5.000000 MHz OUTPUT

Block diagram shows microwave-optical assembly in which a locally generated frequency is compared with the frequency of an atomic transition. The amount and direction of difference are sensed by the phase detector and an error signal applied to correct the local oscillator. *Photograph shows, left to right:* photocell; one of two coils providing a fixed magnetic field; the microwave cavity with diode multiplier on the side, which produces a 6.8-MHz field within the cavity and the enclosed vapor cell; second coil; and lamp stimulating the transition. These optical and microwave components are assembled within magnetic shielding (*not shown*) to reduce effects of the earth's field.

Changes in NBS Radio Broadcasts

Adjustment of WWV, WWVH, and U.S. Navy Time Signals

The National Bureau of Standards and the U.S. Naval Observatory have jointly announced that the clocks of NBS radio stations WWV and WWVH and Navy station NBA, Canal Zone; NPG, San Francisco, California; NPM, Lualualei, Hawaii; NPN, Guam, Mariana Islands; and NSS, Annapolis, Md., were retarded 100 msec at 0000 hours UT on January 1, 1965.

The adjustment is necessary, as in the case of WWVB, because of changes in the speed of rotation of the earth, as determined by astronomical observation. These adjustments are in accordance with an international agreement whereby Universal Time signals are synchronized to about 1 millisecond and are also maintained within about 100 milliseconds of the Universal Time scale, UT2. Participating countries include Argentina, Australia, Canada, Czechoslovakia, France, Italy, Japan, South Africa, Switzerland, United Kingdom, and the United States.

Offset for 1965 Same as for 1964

The Bureau International de l'Heure has announced that the fractional offset from nominal of coordinated transmissions for 1965 will be -150×10^{-10}, the same as for 1964. HF and VLF transmissions from NBS stations, WWV, WWVH, and WWVL, will be offset by this amount from the standard frequencies controlled by the United States Frequency Standard (USFS) maintained by the Boulder Laboratories.

Signal pulses emitted from WWV and WWVH are synchronized to within 1 msec with those from other U.S. and foreign stations and within about 100 msec of UT2.

Transmissions by WWVB are not included in the international agreement.

The difference between the two kinds of time signals is that the time signals from WWVB will be exactly 1 sec apart, whereas those from WWV and WWVH are (intentionally) slightly greater than one second apart. The fractional difference is the figure $+150 \times 10^{-10}$. This small adjustment is made for convenience so that the WWV and WWVH time signals will keep more satisfactorily in step with the UT2 time scale. This is a consequence of the fact that the UT2 scale is related to the rotation of the earth, which proceeds at a slightly slower rate than the scale based on the international second.

Phase Adjustment of WWVB Time Signals

Because of changes in the speed of rotation of the earth on which UT2 is based, on January 1, 1965 the clock at NBS station WWVB (Fort Collins, Colo.) was retarded 200 msec at 0000 hours UT (7:00 p.m. EST December 31, 1964). The phase adjustments insure that the time pulses will remain within about 100 msec of the variable UT2 scale. Thus navigators, who need the UT2 scale to determine their positions, can use these time pulses with just as much confidence as they do those from WWV or WWVH.

new data on
ALUMINUM FATIGUE

Contrary to what has been generally assumed, the presence of water vapor during the initial stages of alternate stressing has no effect on the fatigue strength of aluminum alloy specimens. At the end of this initial period, however, fatigue cracks develop and grow more rapidly in a moist atmosphere than in a dry one. These new findings should have practical applications in the design of aluminum alloy structures, such as air frames, whose fatigue resistance must be accurately known.[1]

Fatigue and Metal Failures

Metal fatigue is the principal cause of the failure of metal parts in service. After protracted cyclic stressing, a crack forms and then grows under continued stressing until the metal piece breaks in two. That the atmosphere has a marked effect on the fatigue process is well known, but the reasons for the effect have not been determined. The present work was undertaken to develop data that would provide a better understanding of the fatigue mechanism.

In the experiments, reversed bending loads were applied to 6061–T6 aluminum alloy specimens. The entire testing machine was enclosed in a cabinet in which the humidity could be controlled and measured. In one series of experiments, the environment was changed from moist to dry after increasing numbers of cycles were run in the moist environment; in a second series, the procedure was reversed and the specimens were stressed first in the dry environment.

If the effect of the water vapor were the same during all stages of the fatigue process, the total life of the specimens in these experiments would be a linear function of the number of cycles in the first environment; however, such was not the case. The results of more than 50 individual tests indicated that the cycles-to-failure depended primarily upon the environment during the latter part of the test. In fact, the data showed that a considerable portion of the metal's fatigue life had been expended before the water vapor had any effect.

Pressure-Sensitive Tape Used

Further experiments were undertaken to determine whether the number of cycles involved in the initial period of stressing (N_R) was the same as the number of cycles required to indicate a fatigue crack (N_C). A recently developed NBS technique provided a ready tool for this part of the study.[2] In this technique, transparent pressure-sensitive tape is applied to the surface of the specimen before it is subjected to reversed bending tests. As soon as a small fatigue crack is formed, gas evolves and forms bubbles under the tape. The bubbles thus serve as a convenient and sensitive indication of the beginning of crack propagation.

At two selected stress levels, a number of determinations were made of the average life of specimens up to the time of crack initiation. Below are given results of these determinations together with the values found for total fatigue life (N_F) at the different stress levels.

(Continued opposite.)

Time-lapse exposures taken with a motion-picture camera during recent tests of a fatigue-stressed aluminum alloy: specimen surface after
—1200×10^3 cycles (gas evolution has not started)
—1280×10^3 cycles (line of small bubbles is circled)
—1350×10^3 cycles (gas evolution at three places)
—1455×10^3 cycles (end of test).
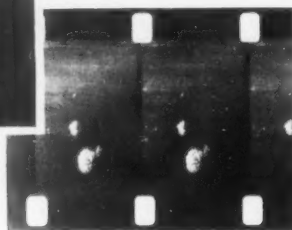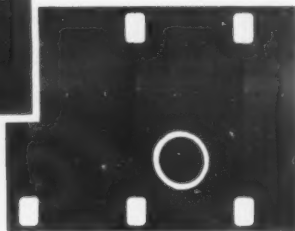
**Research by
John A. Bennett of the NBS
Institute for Materials Research**

Polaron Behavior Studied

Research by
David M. Larsen of the
NBS Institute for Basic Standards

Polarons—electrons surrounded by polarization charge "clouds"—are responsible for charge transport in ionic crystals under certain circumstances. Recent theoretical studies [1] predict the behavior of polarons in strong magnetic fields and suggest possible verifying experiments and methods for observing the behavior. Although polarons have been studied theoretically for about 15 years, there is little experimental evidence with which to check the theoretical models.

Although ionic crystals, such as potassium chloride and silver bromide, normally act as insulators, they will conduct electricity when some of their numerous low-energy electrons are excited to higher energy states (conduction-band states) by the absorption of light. The excited electrons are then free to move through the crystal in response to an applied voltage. Because these high-energy electrons interact strongly with the ions of the crystal lattice, they provide a convenient probe for study of the electron-phonon interaction.

Polarons are formed when the conduction-band electrons surround themselves with polarization charge resulting from the polarizing effect of their coulomb field on the crystal lattice. In effect, the moving free electron is changed into a more complicated excitation corresponding to a moving electron which carries along with it a distortion of the crystal lattice.

In the NBS work, a simple theoretical model of the polaron was considered. The results can be most easily understood if first a discussion is given of the quantum theory of the motion of an electron in a magnetic field in vacuo.

Quantum theory pictures the motion of an electron in a magnetic field in vacuo as a circular motion of frequency v in the plane perpendicular to the direction of the field. (The electron may also move freely in the direction parallel to the magnetic field, but in the present simplified discussion this motion will be ignored.) For a given magnetic field, the radius of the circular orbit can assume only certain discrete values; and for each allowed orbit there is a corresponding discrete electron kinetic energy. The smallest orbit is associated with an energy $(hv/2)$. In general, each successively larger orbit has an energy greater by an amount hv.

It was found that a polaron should behave very much like an electron in vacuo. In particular, in a magnetic field the allowed orbits and energies should be discrete. However, energy differences between successive orbits should decrease slightly as the orbit radius increases.

By measuring these energy differences and comparing them with calculated values, one could determine independently and simultaneously the strength of the electron-lattice polarization force and the electron effective mass for any crystal. These two quantities are the basic parameters in polaron theory and are not yet known for most crystals.

The energy differences are measurable with strong field cyclotron resonance techniques, but such experiments present technical difficulties—the magnetic fields must be quite strong (at least 60,000 oersteds) and the exciting electromagnetic radiation must be in the very far infrared. There have been recent reports of gas lasers that produce lines in the 100-μ region; these would seem to be ideal for inducing transitions between polaron energy states and may provide the best experimental approach to a better understanding of the nature of polarons.

[1] For details, see Energy levels of polarons in a magnetic field, by David M. Larsen, Phys. Rev. 135, No. 2A, A419–A426 (20 July 1964); and Polarons in an electric field, by David M. Larsen, Phys. Rev. 133, No. 3A, A860–A866 (3 Feb. 1964).

Aluminum Fatigue—*Continued*

As in all fatigue testing, considerable scatter was found in the data, but they do show a significant difference between N_R and N_C for the experiments in dry air. It can therefore be said that N_R represents a change in the nature of the fatigue process that definitely precedes the development of fatigue cracks.

Stress amplitude	N_R	Atmosphere	N_C	N_F
183×10^6 N/m² (26,500 psi).	210,000	Dry... Moist..	1,100,000 250,000	1,369,000 423,000
262×10^6 N/m² (38,000 psi).	28,000	Dry... Moist..	35,000 22,000	107,400 48,100

A tentative explanation is proposed for the results obtained in this investigation. During the initial period the metal is apparently undergoing plastic deformation on a microscopic scale, resulting in work-hardening. The deformation, thus uniformly distributed throughout the material, is not sufficiently large to break the protective oxide film on the metal surface. Eventually, however, the metal's capacity to work-harden is exhausted, and work-softening begins. The deformation is then concentrated locally, so that it ruptures the protective film and permits the water vapor to react with the aluminum.

[1] For details, see Changes in the influence of atmospheric humidity during fatigue of an aluminum alloy, by John A. Bennett, J. Res. NBS 68C (Eng. & Instr.), 91 (1964).
[2] Observations concerning metal fatigue, NBS Tech. News Bull. 42, 8 (1958).

Radiant Energy Effects on Asphalt Durability

xenon arc simulates sunlight

Results of a recent study comparing the effects of different radiation sources on asphalt should be of interest to the asphalt and roofing industries. In this study,[1] the effects of solar, carbon-arc, and xenon-arc radiation on coating-grade asphalts were compared. The results show that solar radiation effects are more closely simulated by xenon-arc radiation than by carbon-arc radiation. Therefore, asphalt durability can be determined more accurately by using a xenon-arc weatherometer in place of the presently used carbon-arc weatherometer.

Asphalt is now the most widely used roofing material in the United States. Sunlight causes photo-oxidation in asphalt, and this reaction is the major cause of asphalt degradation. However, studying the reaction is difficult and time consuming, as solar radiation varies almost continuously. For this reason, investigators have sought other radiation sources that could be used in laboratory experiments.

With the development of the carbon arc as a radiation source and the weatherometer to control the test environment, much progress was made in studying photo-oxidation in asphalt. However, use of the carbon arc and weatherometer to simulate natural weather conditions has not been universally accepted because test results vary despite stringent control measures. Consequently, various other radiation sources have been investigated, including the recently developed xenon high-pressure arc.

The xenon arc was found to be the best simulator of sunlight in terms of ultraviolet spectral energy distribution,[2] and the broad violet band of the solar spectrum was found to be a primary cause of photo-oxidation in asphalts.[3] Therefore a study was initiated at NBS to compare the effects of solar, xenon-arc, and carbon-arc radiation on asphalt.

For this study, four coating-grade asphalts were obtained, representing the majority of asphalts used in the United States and having wide durability ranges. Thin-film specimens of the asphalts were prepared and examined. To determine relative rates of oxidation, the infrared absorption spectra of the specimens obtained both before and after irradiation were plotted and compared.

Plots of the reactions for three of the asphalts exposed to solar radiation indicated steady oxidation rates joined by an inflection point and followed by

Interior view of the xenon high-pressure arc weatherometer shows xenon arc surrounded by the specimen rack.

Study by
Keith G. Martin of the
NBS Institute for
Applied Technology

final rupture. The fourth asphalt ruptured prior to the second oxidation rate. The same asphalts reacted in a similar manner when exposed to xenon-arc radiation. However, plots of the reactions of the asphalts irradiated by the carbon arc indicated an induction period, followed by a steady oxidation rate and final rupture. No oxidation occurred during periods of non-irradiation or darkness.

A possible reason for the different oxidation rates of the same asphalts is indicated by the different intensities of broad violet band radiation of the three sources. The maximum solar intensity in the broad violet band, determined in midsummer, was slightly higher than that of the xenon arc. However, the carbon-arc intensity in the broad violet band was 5.2 times greater than that of the xenon arc. The higher intensity of the carbon arc in the broad violet band does not proportionally increase the steady oxidation rate of the asphalts; rather, it appears to reduce the inflection point in the oxidation time curves. This effect varies in magnitude for different asphalts.

Thus, the xenon arc appears to be not only a good simulator of the ultraviolet spectral energy distribution of solar radiation, but also a better simulator of solar radiation on asphalts than is the carbon arc.

[1] For details, see Influence of radiant energy source on asphalt oxidation, by K. G. Martin, J. Appl. Chem. (London), in press.
[2] R. C. Hirt, R. G. Schmidt, N. D. Searle, and A. P. Sullivan, J. Opt. Soc. Am. 50 (1960).
[3] M. Toch, J. Soc. Chem. Ind. 27, 311 (1908).

Solar effects (top), xenon-arc effects (center), and carbon-arc effects (bottom) on four asphalts. Note inflection point separating steady oxidation rates on three of the specimens affected by solar and xenon radiation.

Recorded solar radiation intensity under various conditions at NBS Washington. The relationship of carbon-arc and xenon-arc intensities to solar radiation intensities shows the carbon-arc intensity to be 5.2 times greater than that of the xenon-arc, which is slightly less than the maximum solar intensity.
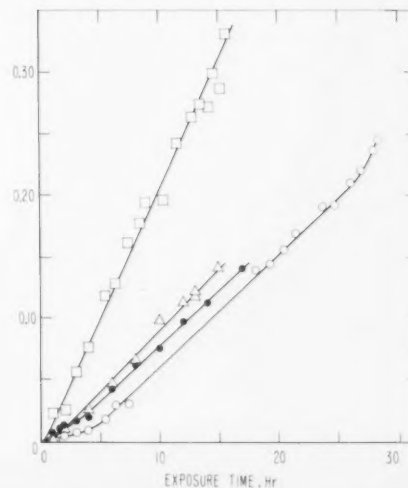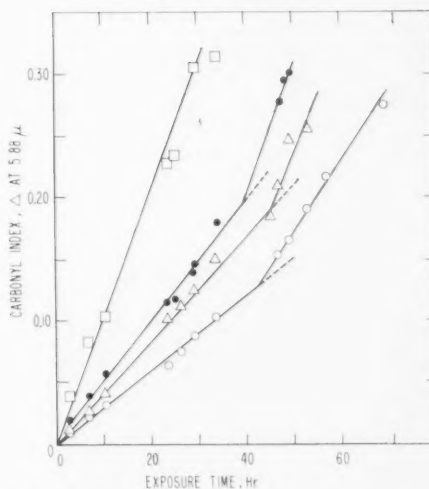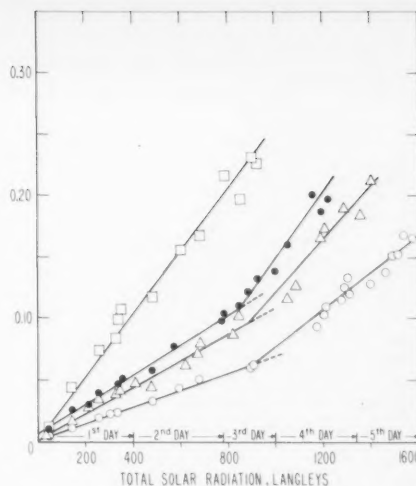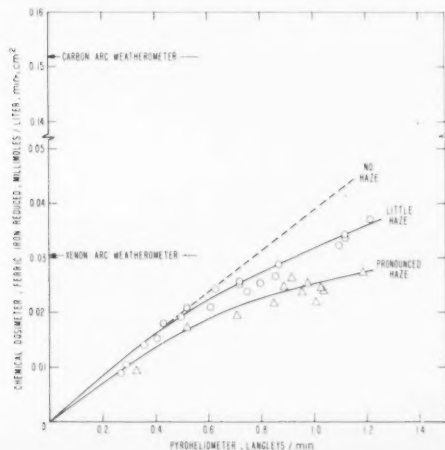
LASER PROVIDES

Meter Measured to 7 Pa

The successful measurement of length with a laser has just been completed at the Bureau. By the use of a laser beam as an interferometric light source, the length of a meter bar was measured with an accuracy better than a part in 10 million. This accomplishment means that the laser—which up to now has had only limited practical applications—has become a scientific tool for achieving dimensional accuracy of a high order.

Conventional light sources, such as krypton 86 or mercury 198 lamps, do not permit direct interferometric measurements of lengths greater than a few decimeters. Hence, successive determinations are made to measure longer lengths, requiring tedious and time-consuming procedures. At the time the laser concept was theoretically developed a few years ago, NBS recognized that its highly coherent light would provide a unique method for interferometrically measuring greater lengths. When the theoretical concept had been reduced to practice, studies were undertaken at the Bureau to adapt lasers to such measurements.

Stability Improved

In early experiments, a helium-neon continuous-wave laser produced interference fringe patterns over an optical path of 200 meters,[1] showing that the use of a laser was feasible for measurements over greater lengths than could be measured with conventional light sources. In these experiments, however, the frequency of the laser oscillation tended to be unstable, so that an accurate interferometric measurement could not be made. A technique was then devised for analyzing laser frequencies;[2] with the information thus obtained, a helium-neon laser with improved stability was designed and built.
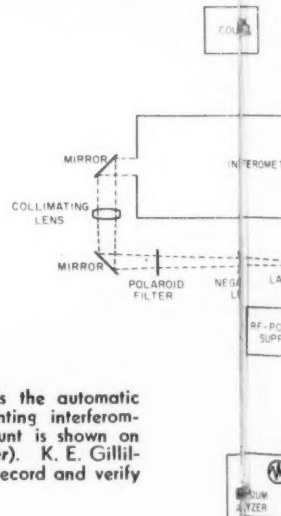
The performance of this laser was then tested in actual length measurements by means of an automatic fringe-counting interferometer that had been developed at the Bureau for measuring line standards up to 1-meter lengths.[3,4] The laser was kept in single-mode operation by adjustment of its rf-power supply, and it was made to operate at or near the center of the red neon spectral line at a wavelength of approximately 632.8 nanometers (6328 Å) by tuning the laser cavity length.

Interferometric Measurements Compared

Since the neon wavelength produced in the laser was not known with sufficient accuracy, it was determined in comparative interferometric measurements. Interference fringe counts were obtained over various portions of a decimeter line standard, first by use of a standard mercury 198 lamp and then by use of the laser. The neon wavelength of this laser was then
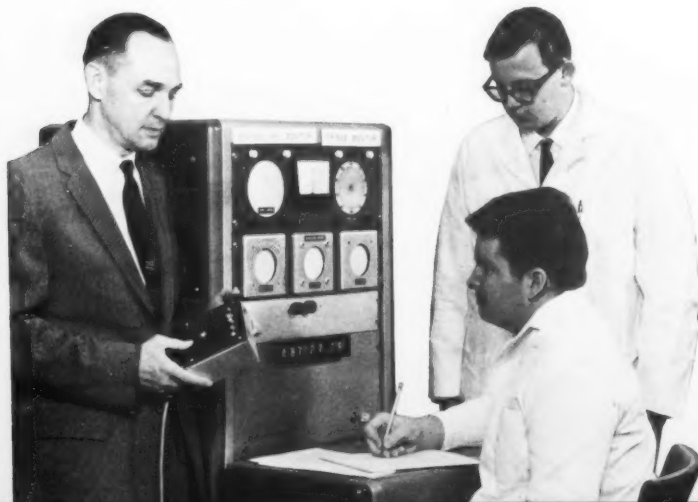
H. D. Cook (*left*) controls the automatic operation of a fringe-counting interferometer (*not shown*). The count is shown on the monitor console (*center*). K. E. Gilliland and R. B. Stephens record and verify data.
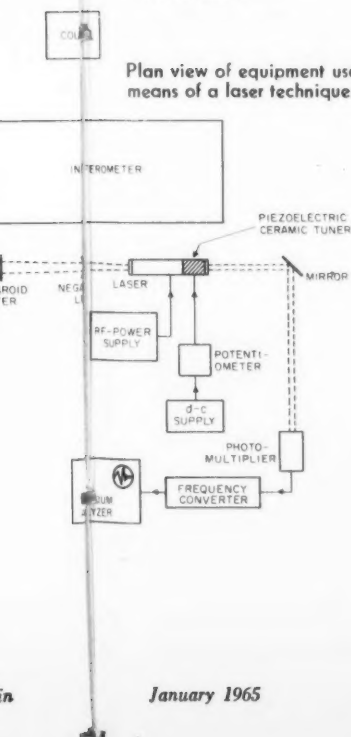
gth measurements
to 7 Parts in 100 Million

Research by
K. D. Mielenz, H. D. Cook,
K. E. Gillilland, R. B. Stephens
of the NBS Institute for
Basic Standards

calculated by use of the internationally accepted value for the mercury 198 wavelength at 436 nm.[5] This calculation showed the neon wavelength to be 632.81983 nm under standard metrological conditions—that is, in air at 20 °C containing 0.03 percent carbon dioxide at standard atmospheric pressure and at 1330 N/m^2 (10 mm Hg) water vapor pressure.

The automatic fringe-counting interferometer, with the laser as a light source, was then used to measure the length of a meter bar in terms of this wavelength. As the meter bar inside the interferometer was moved over its entire length, interference fringes produced by the laser were automatically counted. From the total count of 3 160 460.33 fringes, or half-wavelengths, the length of the meter bar was determined to be 1.000 000 98 m. This length agreed to within 7 parts in 100 million with an independent measurement of 1.000 001 05 m for this meter bar. In addition, measurements of each decimeter graduation on the bar agreed with the independent measurement to better than 0.000 000 5 m.

Plan view of equipment used in measuring one-meter lengths by means of a laser technique.

Future Use

Throughout these experiments, the performance of the interferometer was found to be improved when the laser was substituted for the mercury 198 lamp. With the laser, the contrast of the fringe pattern remained constant over the full length of the meter, thus providing a higher signal-to-noise ratio over the entire path. With mercury 198 light, a fading of the fringes and, hence, an increase of the noise level was noticeable even over the length of the decimeter bar.

The laser was "stable" by virtue of its compact and sturdy design; however, it was "unstabilized" in the sense that no electronic feedback mechanism was used to lock its wavelength output automatically to the center of the neon line. Hence, stabilized lasers with single-mode operation will be used in future experiments to eliminate the need for manual adjustment. Thus accurate length measurements through the use of a laser may ultimately be routinely performed.

[1] Interference fringes with long path difference using He–Ne laser, by T. Morokuma, K. F. Nefflen, T. R. Lawrence, and T. M. Klucher, J. Opt. Soc. Am. 53, 394 (1963) ; and NBS Tech. News Bull. 47, 80 (1963).

[2] A new Fabry-Perot spectrometer for high-resolution spectroscopy and laser work, by K. D. Mielenz, R. B. Stephens, and K. F. Nefflen, J. Res. NBS 68C (Eng. & Instr.), No. 1, 1 (1964) ; and NBS Tech. News Bull. 48, 48 (1964).

[3] An automatic fringe counting interferometer for use in the calibration of line scales, by H. D. Cook and L. A. Marzetta, J. Res. NBS 65C (Eng. & Instr.), 129 (1961).

[4] Lasers for length measurement, by A. G. McNish, Science 146, 177 (1964).

[5] Actions taken by the 12th General Conference on Weights and Measures, NBS Tech. News Bull. 48, No. 12 (1964).

INTERFEROMETER

PIEZOELECTRIC CERAMIC TUNER

LASER

MIRROR

RF-POWER SUPPLY

POTENTI-OMETER

d-c SUPPLY

PHOTO-MULTIPLIER

FREQUENCY CONVERTER

K. D. Mielenz matches the impedance of the rf-power supply to that of the laser.

better paper products through

MICRORADIOGRAPHY

Studies by
Sanford B. Newman and
Donald Fletcher of the
NBS Institute for Materials Research

Better paper products should result from the use of microradiography in studying the relations between paper sheet and its additives. According to recent NBS studies, point-projection microradiography is easier and more rapid than present methods for identifying paper additives, and the optimum amounts and preferred distributions of additives can be determined by comparisons with reference standards.

In the past, investigators have tried using microradiography for research in paper technology and sometimes have been able to reveal the structures and interrelations of fibers in this way. However, microradiography has not been recommended for use as a fabrication control because of cumbersome or costly procedures and because some of the results could be obtained more easily with other methods. Consideration of these earlier results and studies of a survey of papers made for research purposes led the present investigators to conclude that microradiography should be of greatest value in studying the relations of additives to paper.[1] They therefore made a systematic determination of the information derivable from paper specimens using the point-projection method, in which an enlarged image is formed by placing the object close to a point source of x rays (see below). The apparatus used at NBS included a two-lens electromagnetic x-ray microscope having the gun and lenses mounted vertically with the objective above. Specimens were placed on spacers supported 1 or 2 mm above the target. Aluminum targets of 3 and 9 μ thickness were employed. Exposure times were under 5 min, and tube current was 20 μA.

Various Additives

Glue. The distribution and location of adhesive in paper products often affect their structural characteristics. Penetration of the glue in such products as gummed tapes and stamps is an important factor in performance.

Corrugated paperboard was examined to determine the distribution of the adhesive, which was found to follow several patterns. A kraft gummed tape was also viewed. Bubbles and other inhomogeneities were visible in some adhesive layers of both products. The area of glue penetration into the paper could be seen clearly. Where penetration was poor or practically nonexistent, the bond of the adhesive to the substrate usually was poor.

Titanium dioxide. Titanium dioxide pigments are used as paper fillers primarily for their opacifying and brightening effects. The final state of aggregation in the sheet is dependent on the papermaking operation and is difficult to predict. Samples of paper having percentages of titanium dioxide varying from 0.75 to 6 added to the stock were studied. Similar samples having 2 percent of rosin size in addition to the titanium dioxide were also considered. Samples with only rosin added and samples having no additives were included as controls.

Microradiographs of all samples containing titanium dioxide revealed opaque aggregates. Since these aggregates were lacking in papers without any additive, as well as in those with only rosin added, the aggregates were assumed to be titanium dioxide. The number of
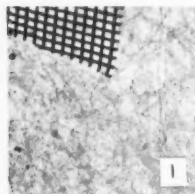
Left: Paper with varying amounts of titanium dioxide. (1) 0.75 percent titanium dioxide, (2) 6 percent titanium dioxide. Center: Paper with 5 percent added clay. Right: Paper with varying amounts of titanium dioxide and rosin, (3) 0.75 percent titanium dioxide, 2 percent rosin, (4) 2 percent titanium dioxide, 2 percent rosin. pH of papers was adjusted to 5.0 using alum. Grids contain 500 wires per inch. Aluminum target; 15 kV.
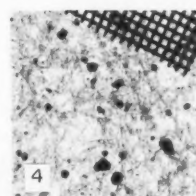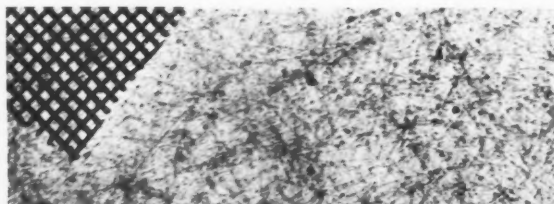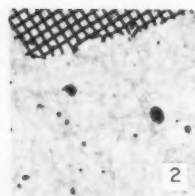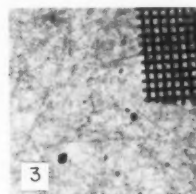
visible aggregates increased with increasing percentage of added titanium dioxide, but size range of the aggregates did not appear to change with changing titanium dioxide content. The number of aggregates increased more rapidly at higher levels of added titanium dioxide when rosin was also present. Apparently rosin size promoted agglomeration.

There seems little doubt that aggregates of titanium dioxide are visible in microradiographs of papers prepared for this study when as little as 0.75 percent of the compound has been added to the paper-making ingredients. The surface appearance of the sheet is probably not greatly affected by these aggregates, for not only are many of them in planes not in contact with the surface, but they occupy only a small portion of the area of the sheet. Since, however, small amounts of titanium dioxide do affect the surface brightness of paper, it is logical to assume that a portion of the titanium dioxide is finely dispersed and that this portion efficiently covers a large surface area, even though it cannot be resolved in the microradiographs. Surface brightness is, then, dependent chiefly on that fraction of the additive which has a particle size below the range of the x-ray microscope. Microradiography, be-cause it reveals the relatively ineffective fraction of agglomerated filler, provides a convenient technique for determining the range in which additional amounts of titanium dioxide fail to contribute proportionate improvement in surface properties.

Clay. Clay is added to paper as a filler to improve the smoothness, gloss, and printability of the sheet. It decreases the bulk and softens the sheet, but interferes to some degree with the sizing. Clay also improves the brightness and opacity of paper. As clay is much cheaper than titanium dioxide, the latter is used only in the best grade of paper where extreme whiteness is desired.

In the NBS study it was found that the number of aggregates of added clay increased with the amount of additive. The size range of aggregates was much more limited than for titanium dioxide.

[1] *For details, see* Soft x-ray microscopy of paper, *by Sanford B. Newman and Donald Fletcher, TAPPI* **47**, No. 4, 177–180 (1964).

(a) Radiomicrographs of glue areas in corrugated paperboard (aluminum target; 15 kV). B and G, fairly homogeneous layers of glue; C, D, and F, more or less continuous lines. C retains outlines of bubbles present at some stage of application of glue; A shows both line and bubble patterns. (b) Radiomicrograph cross section of a kraft gummed tape. Dark arrows indicate a layer of glue that is clear of fibers but contains bubbles and other inhomogeneities. Light arrows point to dark band that marks depth of glue penetration.
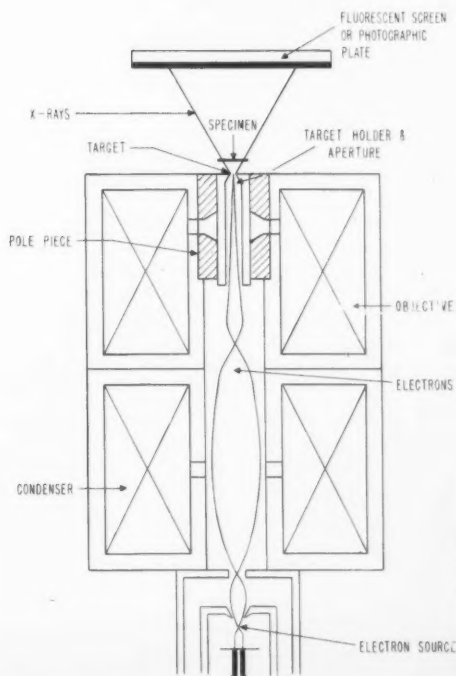
Left: Schematic diagram of the point-projection x-ray microscope.

Below: Overall view of the equipment. Lenses and gun, *foreground;* vacuum pumps, gages, and controls in cabinet, *left;* electrical high-tension, bias, and filament supplies in rack, *right.*
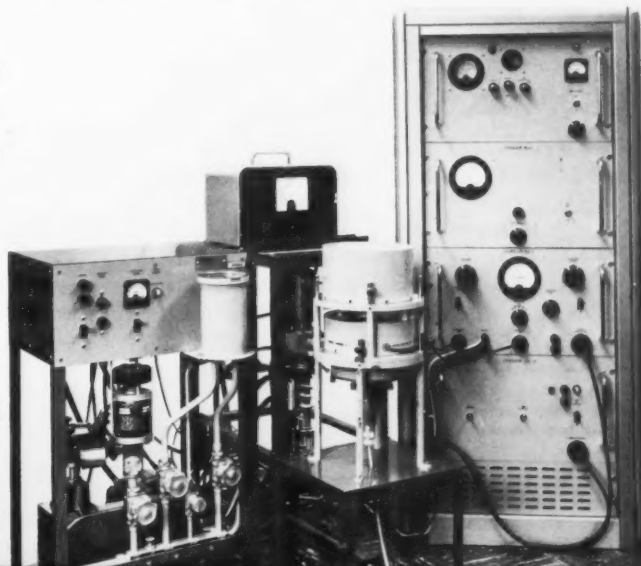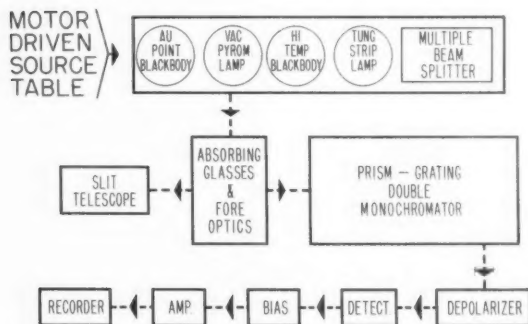
accuracy of
SPECTRAL RADIANCE CALIBRATIONS
increased

new instrument extends range

**Research by
H. J. Kostkowski, D. E. Erminy,
and A. T. Hattenburg of the
NBS Institute for Basic Standards,
with partial support from NASA.**

A fivefold improvement in the accuracy of spectral radiance calibrations between 800 and 250 nm (8000 and 2500 Å) is possible with a recently developed spectroradiometer. The new instrument also extends the calibration range down to about 200 nm.

High accuracy in spectral radiance determinations is important to pyrometry, where measurements at various wavelengths are desired; to spectroscopy, where gas temperatures and transition probabilities are determined; and to precise optical measurements of reflectance, transmittance, and emissivity. Up to now, the accuracy of calibration of spectral radiance standards has been inferior to that of standards representing almost any other widely used physical quantity. At 800 nm, the uncertainty was about 3 percent; and at 250 nm, 8 percent. The Bureau's new spectroradiometer has an estimated uncertainty of 0.3 percent at 800 nm and 1.5 percent at 210 nm. The uncertainties associated with gas-filled tungsten strip lamps calibrated by this instrument will possibly be twice these amounts because of instabilities of the lamps.

The most significant contribution to the increased accuracy of the new instrument is the high accuracy with which the temperature of a highly stable blackbody is determined by various elements that constitute an internal photoelectric optical pyrometer. The extension in range results primarily from the fact that the blackbody can operate routinely up to 2700 °C.

The spectroradiometer consists of a double monochromator with a photomultiplier detector and associated electronics, a stable high-temperature blackbody, and a vacuum pyrometer lamp. The internal pyrometer portion of the spectroradiometer is calibrated relative to the International Practical Temperature Scale using another blackbody maintained at the freezing temperature of gold (the gold-point blackbody), a multiple beam-splitter device,[1] and methods developed for optical pyrometry.

In using the spectroradiometer, the high-temperature blackbody is adjusted until its spectral radiance at a particular wavelength is equal to that of the test source (e.g., tungsten strip lamp). This spectral radiance is then determined with Planck's radiation equation using the blackbody temperature as found with the internal pyrometer.

The high-temperature blackbody is a graphite tube heated electrically in an argon atmosphere. By careful consideration of the geometry, an emissivity of 0.998 has been achieved. Temperature can be controlled so that variations in radiation are less than 0.1 percent.

Efforts are being made to standardize the calibration procedure, to extend the wavelength range to 2.5μ, and to apply the calibration to various types of tungsten strip lamps and to the low-current carbon arc. In order to complete this work as soon as possible, only a limited number of special calibrations are being offered at this time. Priority will be given to persons who require calibrations below 250 nm and to those whose research problems exhibit a need for a smaller uncertainty in spectral radiance than is available commercially (about 5 percent). Such persons are invited to write to Dr. H. J. Kostkowski, Temperature Physics Section, National Bureau of Standards, Washington, D.C., 20234.

Above: Major features of the spectroradiometer and of associated temperature calibration apparatus.

[1] Scheme for obtaining integral and fractional multiples of a given radiance, by Diamond E. Erminy, *J. Opt. Soc. Am.* **53**, *No. 12, 1448–1449* (1963).

Nineteenth Annual Calorimetry Conference

The 19th Annual Calorimetry Conference was held October 13 to 16, 1964, under the joint sponsorship of the Bureau and the National Naval Medical Center (Bethesda, Md.). Each organization was in turn host to six of the twelve Conference sessions. The purpose of the Conference is to review and exchange current thermodynamic and thermochemical data and information on calorimetric techniques, and to encourage cooperative efforts for new studies. A subject of special emphasis in this Conference was biochemical investigations. The sessions, at which 52 technical papers were presented, were attended by more than 200 delegates, including 12 from foreign countries.

At the opening technical session, which was held at the Bureau, the delegates were welcomed by Dr. R. D. Huntoon, Director of the NBS Institute for Basic Standards, who expressed the hope that the Conference would meet in Washington on a more frequent basis.

The main conference address, the Huffman Memorial Lecture (in honor of Hugh M. Huffman, founder of the Conference) was presented by J. M. Sturtevant of Yale University. Professor Sturtevant, a pioneer in biochemical studies, reported on his current work on the heats of hydrolysis of peptide and amide bonds, which has an important application to problems in energetics of protein biosynthesis.

Instrumentation was the principal topic at the second technical session. G. T. Furukawa described a specially designed automatic bridge for platinum resistance thermometry which measures resistances up to 500 ohms to the nearest 0.00001 ohm.

Studies on vapor pressure were considered at the Conference's third session. P. W. Gilles (Univ. of Kansas) and J. M. Leitnaker (Baker Univ., Baldwin, Kans.) described the usefulness of vaporization experiments in obtaining thermodynamic data, with particular attention to zirconium diboride thermodynamics.

The last session of the opening day was devoted to the presentation of several papers on high-temperature thermodynamics of metals and ceramics, and on the interpretation and limitations of the existing experimental methods.

On the second morning of the Conference at NBS, presentations relating to low-temperature calorimetry and reaction calorimetry were held at concurrent sessions.

The second group of six sessions opened that afternoon at the National Naval Medical Center with welcoming addresses by Capt. J. R. Seal (Commanding Officer, Naval Medical Research Institute) and Rear Adm. C. B. Galloway (Commanding Officer, National Naval Medical Center). T. H. Benzinger (Naval Medical Research Institute), in his introductory remarks, underlined the Conference emphasis on calorimetric studies in biochemistry.

The theme of the session, "The Driving Forces of Life," was developed by R. E. Davies (Univ. of Pennsylvania) in his discussion of the liberation and utilization of energy in life processes which emphasized the mechanism of muscle contraction. Continuing this theme, L. Kiesow (National Naval Medical Center) outlined the steps in the assimilation of energy for biosynthesis.

The final session of the second day was devoted to papers on the application of radiation calorimetry to the measurement of radiation doses and the quantitative determination of radioactive materials. The opening paper, given by S. R. Gunn (Univ. of California), was a comprehensive review of calorimeters used for the study of radiation processes.

On the third day of the Conference, the ninth and tenth sessions covered the performance and use of specially designed calorimeters, techniques of heat measurement, the determination of sample purity, and the interpretation of transitions observed in inorganic compounds and metals.

A business meeting, chaired by G. T. Armstrong, was held at the conclusion of the tenth session. A resolution was adopted to request that the Bureau make available standard samples of aluminum oxide (used as a standard in heat-capacity measurements) and of *tris* (hydroxymethyl)aminomethane, THAM (to be used as a standard in reaction calorimetry).

Session eleven dealt principally with thermodynamic studies of electrolytic solutions. K. P. Mishchenko (Leningrad Technological Institute of the Cellulose and Paper Industry, Leningrad, U.S.S.R.) presented the results of aqueous and nonaqueous solution calorimetry experiments. T. F. Young, Y. C. Wu, and W. L. Groenier (Argonne National Laboratory) reported highly precise measurements of the heats of dilution of sulfuric acid at low concentrations and showed the results to be in satisfactory agreement with theoretical calculation of the heats of dilution of sulfuric acid in dilute solutions. This work greatly reduces the uncertainties of extrapolation to infinite dilution.

At the concluding session, several papers on reaction calorimetry of solutions, flame calorimetry, and a highly sensitive diphenylether Bunsen calorimeter were featured.

Polymer Adsorption on Surfaces

Nature of Plastic-Surface Bonding

Polymer adsorption is an important factor in the fabrication of numerous composites for military and commercial applications. These include glass-fiber reinforced plastics, tires, most adhesive joints, and many protective coatings. Although the adsorption of polymers has considerable industrial significance, little is known about the way in which it occurs.

For some time, research to obtain a better understanding of the nature of polymer adsorption has been in progress at the NBS Institute for Materials Research. Some of this work was sponsored by the Office of Army Research and the Bureau of Naval Weapons. Two of the principal problems to be resolved are the shape of the polymer molecule—that is, its conformation when it is attached to the surface—and the number of contacts the molecule makes with the surface. The number of contacts of the polymer molecule is of critical importance in evaluating the "strength" of the attachment of the plastic to the surface. The extension of the attached molecule away from the surface is of importance in evaluating the interaction of the attached molecule with other molecules in the bulk plastic. The information developed from the recent NBS research should therefore be useful in the improvement of composites using plastic materials.

Ellipsometry Measurements

In one series of experiments, an ellipsometer was employed to study the extension of an adsorbed polymer molecule from the surface. In this instrument, changes in the state of polarization of light after reflection from a film-covered surface are measured and used to calculate the thickness and refractive index of the film.[1,2] The system studied was polystyrene adsorbed from cyclohexane on chrome surfaces.

The ellipsometric measurements showed that at room temperature and at concentrations up to about 2 mg/ml, the thickness of an adsorbed film of a 76,000 molecular weight polymer increased with increasing solution concentration. However, a root-mean-square average thickness of approximately 115 Å was obtained over most of the concentration range.[3]

Studies were also carried out for other molecular weight polymers. For example, a rms average thickness of 290 Å was obtained for the adsorbed film of a 537,000 molecular weight polystyrene on a chrome surface from a 0.23 mg/ml cyclohexane solution. These values are close to the dimensions of the polymer molecules in solution. Hence, it appears that under the conditions of maximum adsorption from ideal solutions, the conformation of the molecule on the surface is similar to that of a random coil.

In these experiments, it was also possible to calculate the concentration of polymer in the adsorbed polymer film. This concentration for the 76,000 molecular weight material was found to be about 12 percent over most of the concentration range. From the thickness measurements and the measured difference in refractive index of a bare surface and a film-covered surface, the amount of adsorbed polymer was determined to be approximately 2×10^{-4} mg/cm² for this polymer.

The ellipsometric technique was also used to study thin films on transparent surfaces.[4] In one of these investigations,[5] the thicknesses of adsorbed "glass finishes"—vinyl *tris*(2 methoxyethoxy)silane and gamma aminopropyltriethoxysilane—on glass prisms were measured. It had previously been assumed that the organic molecules of these finishes were individually adsorbed on a glass surface. The results of this work showed, however, that polymerization occurs either in solution or at the interface and that more complex polymer molecules, sometimes forming films up to 200 Å thick, were adsorbed.
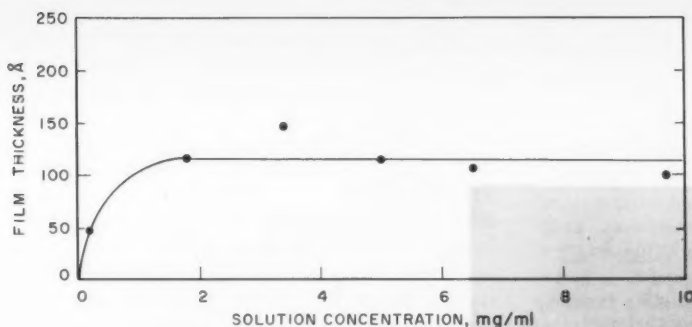
Radioactive Polymers

Radioactive polymers were used to study polymer adsorption in a second series of experiments.[6] Tritium-labeled styrene was first anionically polymerized into fractions of 76,000 and 38,000 molecular weights. The rates of adsorption of these fractions from cyclohexane on chrome surfaces were then determined by means of a windowless Geiger counter equipped with an automatic changer. The technique permitted measurements of the amount of adsorbed polymer from low solution concentrations of from 10^{-1} to 10^{-4} mg/ml.

The measurements showed that the adsorption rates depended directly on both solution concentration and molecular weight. At the 10^{-4} mg/ml concentration, maximum adsorption occurred in less than 4 hr for the 38,000 molecular weight sample but took 24 hr for the 76,000 molecular weight sample.
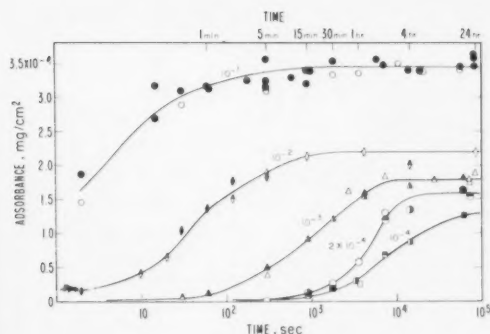
From the results obtained with both molecular weight samples, it appears that the rates of two fundamental processes govern the rate of adsorption for polymer molecules:

(1) a rate for the initial attachment of the polymer at certain points on the surface, and

(2) a rate for the spreading of the polymer on the surface, causing additional attachments.

The rate of initial contact depends partly on diffusion of the polymer to the surface and therefore on the polymer concentration in solution. The degree of spreading of a polymer molecule, that is, the number of

FILM THICKNESS, Å
250
200
150
100
50
0

0   2   4   6   8   10
SOLUTION CONCENTRATION, mg/ml

Research in progress at the NBS Institute for Materials Research

TIME
1 min   5 min 15 min 30 min 1 hr   4 hr   24 hr

ADSORBANCE, mg/cm²
3.5x10⁻⁶
3.0
2.5
2.0
1.5
1.0
0.5

10   10²   10³   10⁴   10⁵
TIME, sec
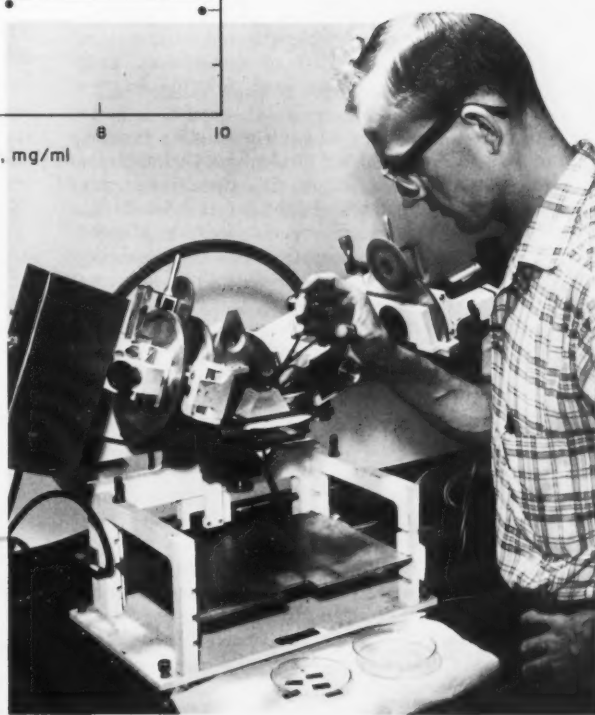
Top left: Measurements carried out by an ellipsometric technique showed that the root-mean-square average film thickness was about 115 Å over most of the concentration range. *Top right:* Daniel J. Tutas inserts a specimen into cell on the ellipsometer stage prior to taking a reading. *Lower left:* Warren H. Grant uses a Geiger counter to detect the amount of adsorbed polymer on chrome. The chrome specimens (two may be seen in the holders at the front of the instrument) had previously been exposed to tritium-labeled polystyrene. *Lower right:* Radiotracer techniques were used to measure adsorbance of tritium-labeled polystyrene on chrome from extremely low concentration solutions. The numbers on the curves in this graph represent the concentrations in mg/ml. The different symbols given for each concentration represent separate runs.

contacts each chain makes with the surface, depends on the surface area available to it before it is blocked by a neighboring molecule.

Infrared Measurements

Infrared measurements were used in a third series of experiments to determine the amount of polymer adsorbed on glass powder.[7] Six low molecular weight fractions (from 970 to 6250) of a polyester, poly (ethylene o-phthalate), were used for the experiments.

The infrared absorption of various solution concentrations was first determined at the 5.8μ carbonyl absorption band. Each solution was then thoroughly mixed with glass powder in a tube for at least 20 hr. After the elapsed absorption time, the glass was allowed to settle, and carbonyl absorption of the remaining solution was again determined. Adsorption isotherms were established at 50 °C and at 0 °C. From the absorption determinations it was found that larger adsorbances occurred at the higher temperature.

Cycling the temperature in these experiments from 0 to 50 °C and from 50 to 0 °C resulted in complete reversibility of adsorbance. In subsequent experiments, however, when the glass powder was first outgassed and heated before mixture with polymer solution, lowering the temperature resulted in a decrease in adsorbance, but an increase in temperature did not result in an increase in adsorbance.

The different results obtained for the treated and untreated glass surface were attributed to an adsorbed water layer on the untreated glass and an increased number of silanol groups on the treated glass. The one-directional "reversibility" was also explained by the following changes in polymer molecular configuration.

When the temperature was lowered, desorption occurred as required for equilibrium. The remaining polymer molecules then rearranged themselves in order to occupy the vacated sites. When the temperature was raised, each polymer molecule occupied more area than could be allowed under these new equilibrium conditions, so some polymer had to be desorbed before additional polymer could be readsorbed in a somewhat different polymer conformation. It seems that the desorption required to achieve this new conformation proceeds at an extremely slow rate, resulting in an apparently irreversible condition.

[1] Measurement of the thickness and refractive index of very thin films and the optical properties of surfaces by ellipsometry, by F. L. McCrackin, E. Passaglia, R. R. Stromberg, and H. L. Steinberg, J. Res. NBS **67A** (Phys. & Chem.), 363 (1963).

[2] For the present state of the art, see Proceedings of the Symposium on the Ellipsometer and Its Use in the Measurement of Surfaces and Thin Films, described on p. 19.

[3] Thickness of adsorbed polystyrene layers by ellipsometry, by R. R. Stromberg, E. Passaglia, and D. J. Tutas, J. Res. NBS **67A** (Phys. & Chem.), 431 (1963).

[4] Optical properties of thin films on transparent surfaces by ellipsometry; Internal reflection for film-covered surfaces near the critical angle, by E. Passaglia and R. R. Stromberg, J. Res. NBS **68A** (Phys. & Chem.), 601 (1964).

[5] Studies of the thickness of adsorbed glass finishes by ellipsometry, by D. J. Tutas, R. R. Stromberg, and E. Passaglia, Soc. Plastics. Eng. Trans. **4**, 256 (1964).

[6] Rates of adsorption and desorption of polystyrene on chrome surfaces, by R. R. Stromberg, W. H. Grant, and E. Passaglia, J. Res. NBS **68A** (Phys. & Chem.), 391 (1964).

[7] Reversibility of polyester adsorption on glass, by R. R. Stromberg and W. H. Grant, J. Res. NBS **67A** (Phys. & Chem.), 601 (1963).

New NBS Film:

Mixing Nonhomogeneous Air Streams

A new 6-minute film of interest to engineers concerned with measuring the properties of moving air has been produced by the Bureau and is available for viewing by any interested group. Entitled "Mixing Non-Homogeneous Air Streams," the motion picture is in 16-mm color with sound.

In the testing and rating of air flow equipment, it is important that the air be thoroughly mixed with respect to temperature and humidity; otherwise, a very large number of measurements must be made and the observed values must be weighted to arrive at an accurate average. Also important are the space required for the mixing device to perform its function, and the pressure drop caused by the device.

The film demonstrates a small-scale apparatus designed and used at the Bureau to make preliminary evaluations of air-mixing devices during their design and development period.

The film shows chemical smoke and air flowing through the mixing devices. In this way temperature and humidity variations in the air stream are simulated. Such flow visualization provides information for selection of the designs that later are given more comprehensive evaluation in a large test apparatus.

The film is of interest to air-conditioning, heating, and refrigerating engineers, and to any group interested in the problems of air flow measurement. A print can be borrowed at no cost other than payment of postage and insurance. For information, write to the Office of Technical Information, National Bureau of Standards, Washington, D.C., 20234. The same office will answer queries as to purchase of prints.

Publication and Conference Briefs

Radio Science Features . . .

. . . Non-Linear Conference Papers

The January issue of *Radio Science,* published by the Bureau in cooperation with URSI, will be devoted to selected papers from the Conference on Non-Linear Processes in the Ionosphere, which was held at the NBS Boulder (Colo.) Laboratories, December 16 and 17, 1963. Guest editors for the issue are Dr. Donald H. Menzel, Harvard College Observatory, and Dr. Ernest K. Smith, Central Radio Propagation Laboratory, NBS. The conference attracted radio scientists from Government, universities, and industrial laboratories in the United States, Canada, Australia, and Italy.

The complete conference proceedings are available in NBS Technical Note 211, a six-volume, 664-page publication, edited by Menzel and Smith.

. . . "Waves-in-Plasma" Papers

The February issue of *Radio Science* will carry 13 papers on "Waves in Plasma" by international leaders in the field, according to Dr. James R. Wait, editor of the Journal. Additional papers on the same subject will appear in later issues.

With the advent of manned space vehicles and the need for communications during reentry, the consequences of the plasma sheath become increasingly important. These featured papers investigate various aspects of the related problems. Included in the list of topics are the following: the alleviation of blackout effects; radiation characteristics of satellite-borne antennas which are immersed in a plasma; effects of surface waves at the interface between the surface of the vehicle and the plasma; ray theory for deducing the profile of the electron density variation in the transverse direction; driving point impedance of an antenna immersed in a plasma; and modifications required to generalize the classical theory of wave propagation in a plasma.

The following authors contributed to the February issue's special section: Dr. Bachynski, RCA Research Laboratories, Canada; Prof. Felsen, Polytechnic Institute of Brooklyn; Drs. Adachi and Mushiake, Tohoku University, Japan; Prof. Cullen, Sheffield University, England; Dr. Galejs, Sylvania Electric Products; Dr. Budden, Cambridge University, England; Dr. Mentzoni, Sylvania Electric Products; Dr. Heisler, University of Sydney, Australia; Drs. Lee, Peters, and Walter, Ohio State University; Dr. Chen, Michigan State University; and Dr. Wait, NBS Boulder.

1963 Ellipsometry Symposium Proceedings

The detailed study of surfaces and thin films overlaying them is becoming increasingly significant in many fields of science. Because of this significance, the technique of ellipsometry for the study of surfaces and thin films has been further developed and applied to such problems as the study of metal surfaces and oxidation and corrosion processes on them, adsorption phenomena on semi-conductor and metal surfaces both from the vapor phase and from solution, electrochemical phenomena, and the thin films now used in solid-state electronics. Application has also been made to the study of biological processes such as blood coagulation.

NBS Miscellaneous Publication 256, *Ellipsometry in the Measurement of Surfaces and Thin Films,* edited by E. Passaglia, R. R. Stromberg, and J. Kruger, contains the latest developments, techniques, and theories of ellipsometry to assist the expert. It also presents a broad historical approach to the subject, which should be of great interest to new workers in the field.

Particle Accelerator Conference March 10-12, 1965

This Conference will provide an opportunity for the discussion of current problems in the design of accelerators and associated research equipment. The Conference, sponsored by the American Physical Society, the Institute of Electrical and Electronics Engineers, the U.S. Atomic Energy Commission, and the Bureau, will be held March 10 to 12, 1965, at the Shoreham Hotel in Washington, D.C.

Many aspects of engineering problems of accelerators and related devices will be covered in the invited and contributed papers of the Conference. Sessions will include such topics as

—ion sources; high-voltage technology and injection

—high-power rf sources; accelerating rf structures

—accelerator magnets and power supplies; beam dynamics problems

—accelerator component controls and automation controls

—beam-sensing and -handling techniques

—future accelerators.

Questions concerning details of the Conference should be directed to E. H. Eisenhower, National Bureau of Standards, Washington, D.C., 20234.

Conference on Phenomena in the Neighborhood of Critical Points

The Bureau, aided by a grant of the National Science Foundation, is sponsoring a conference to discuss phenomena in the neighborhood of critical points. The conference is scheduled for April 5 through 9, 1965 at the Bureau in Washington, D.C.

The conference is intended to bring together experimentalists and theorists who are using diverse methods to study critical phenomena in a variety of phase transitions. It will provide a forum for discussing successes and shortcomings of current theory and for presenting new results and approaches. Some of the subject areas will be liquid-vapor, liquid-mixture, magnetic, solid-solution, and order-disorder transitions; light, x-ray, and neutron scattering; and ultrasonic propagation.

The organizing committee members are Melville S. Green, Chairman (NBS), Elliott Montroll (Institute for Defense Analysis, George B. Benedek (MIT),

Michael Fisher (University of London), and Cornelius J. Pings (California Institute of Technology). Further information may be obtained from the Chairman. Correspondence should be directed to

Dr. M. S. Green, Chief
Statistical Physics Section
National Bureau of Standards
Washington, D.C. 20234.

Publications of the National Bureau of Standards

Periodicals

Technical News Bulletin, Vol. **48**, No. 11, December 1964. 15 cents. Annual subscription: $1.50, 75 cents additional for foreign mailing. Available on a 1-, 2-, or 3-year subscription basis.

CRPL Ionospheric Predictions for March 1965. Three months in advance. Number 24, issued December 1964, 25 cents. Annual subscription: $2.50, 75 cents additional for foreign mailing. Available on a 1-, 2-, or 3-year subscription basis.

Journal of Research of the National Bureau of Standards
 Section A. Physics and Chemistry. Issued six times a year. Annual subscription: Domestic, $4; foreign, $4.75. Single copy, 70 cents.
 Section B. Mathematics and Mathematical Physics. Issued quarterly. Annual subscription: Domestic, $2.75; foreign, $2.75. Single copy, 75 cents.
 Section C. Engineering and Instrumentation. Issued quarterly. Annual subscription: Domestic, $2.25; foreign, $2.75. Single copy, 75 cents.
 Section D. Radio Science. Issued monthly. Annual subscription: Domestic, $9; foreign, $11.50. Single copy, $1.00.

Current Issues of the Journal of Research

J. Res. NBS **69A** (*Phys. and Chem.*), No. 1 (*Jan.–Feb. 1964*). Heat of decomposition of sodium and potassium chlorate. A. A. Gilliland and D. D. Wagman.

Application of precise heat-capacity data to the analysis of the temperature intervals of the NBS–1955 and the International Practical Temperature Scales in the region of 90 °K. G. T. Furukawa and M. L. Reilly.

Heat capacity and thermodynamic properties of beryllium aluminate (chrysoberyl), $BeO \cdot Al_2O_3$, from 16 to 380 °K. G. T. Furukawa and W. G. Saba.

Thermodynamics of the ternary system: water-sodium chloride-barium chloride at 25 °C. R. A. Robinson and V. E. Bower.

Compressibility of eleven inorganic materials. C. E. Weir.

Determination of the intermolecular entanglement coupling spacings in polyisoprene by viscosity measurements. L. J. Fetters.

Electrical conductivity of dilute solutions of "sea water" from 5 to 50 °C. C. G. Malmberg.

Preparation of a carbonate-free complex calcium aluminate. H. A. Berman.

Synthesis and thermal stability of *bis*(8-hydroxyquinoline)-Schiff base coordination polymers. E. Horowitz and T. P. Perros.

Atomic absorption spectrum of praseodymium (Pr I). R. Zalubas and M. Wilson.

J. Res. NBS **69C** (*Eng. and Instr.*), No. 1 (*Jan.–Mar. 1965*). Two picnometers of increased convenience and precision. A. Johnson.

Construction of a Michelson interferometer for Fourier spectroscopy. H. N. Rundle.

The National Bureau of Standards gas thermometer II. Meas-

urement of capacitance to a grounded surface with a transformer ratio-arm bridge. L. A. Guildner and R. E. Edsinger.

An adiabatic calorimeter for the range 10 to 360 °K. K. F. Sterrett, D. H. Blackburn, A. B. Bestul, S. S. Chang, and J. Horman.

A rugged null-type pressure transducer of high reproducibility for accurate gas phase PVT measurements. M. Waxman and W. T. Chen.

Detection and damping of thermal-accoustic oscillations in low-temperature measurements. D. A. Ditmars and G. T. Furukawa.

NBS free-air chamber for measurement of 10 to 60 kV X-rays. P. J. Lamperti and H. O. Wyckoff.

A compensated solenoid giving a uniform magnetic field over a large volume. C. Snow and R. L. Driscoll.

Evaluation of a microwave phase measurement system. D. A. Ellerbruch.

Polarographic analysis of titantium (IV)—EDTA complex: application to paint pigments. H. W. Berger and B. C. Cadoff.

Soil resistivity as related to underground corrosion and cathodic protection. W. J. Schwerdtfeger.

Radio Sci. J. Res. NBS/URSI **69D**, *No. 1, (Jan. 1965)*.

Some problems of ionospheric nonlinearities. D. H. Menzel.

Some nonlinear phenomena in the ionosphere. V. A. Bailey.

An experimental study of gyro interaction in the ionosphere, at oblique incidence. F. H. Hibberd.

On some nonlinear phenomena in the ionospheric plasma. P. Caldirola and O. De Barbieri.

Ionospheric cross modulation: a microscopic theory. D. Layzer and D. H. Menzel.

VLF noise bands observed by the Alouette I satellite. J. S. Belrose and R. E. Barrington.

Excitation of optical radiation by high power density radio beams. L. R. Megill.

Alteration of the electron density of the lower ionosphere with ground-based treansmitters. P. P. Lombardini.

Collision effects in hydromagneto-ionic theory. H. K. Sen. and A. A. Wyller.

Electromagnetic wave reflection from an oscillating, collision-free magneto-ionic medium. O. E. H. Rydbeck.

Nonlinear propagation of electromagnetic waves in magneto-plasmas. II. (an invited abstract). M. S. Sodha and C. J. Palumbo.

Other NBS Publications

Ellipsometry in the measurement of surfaces and thin films, Symposium Proceedings, Washington 1963, ed. E. Passaglia, R. R. Stromberg, and J. Kruger, NBS Misc. Publ. 256 (Sept. 15, 1964), $2.25.

Standard Reference Materials: Metallographic characterization of an NBS spectrometric low-alloy steel standard, R. E. Michaelis, H. Yakowitz, and G. A. Moore, NBS Misc. Publ. 260–3 (Oct. 22, 1964), 20 cents.

Quarterly radio noise data—September, October, November 1963, W. Q. Crichlow, R. T. Disney, and M. A. Jenkins, NBS Tech. Note 18–20 (Oct. 23, 1964), 50 cents.

Calculation of sunrise and sunset times at ionospheric heights along a great circle path, A. H. Brady and D. D. Crombie, NBS Tech. Note 209 (Nov. 8, 1964), 20 cents.

A program for plotting circles of constant overpressure around targeted points, M. L. Joel and D. D. Lottridge, NBS Tech. Note 249 (Oct. 28, 1964), 40 cents.

Research on crystal growth and characterization at the National Bureau of Standards, January to June 1964, ed. H. F. McMurdie, NBS Tech. Note 251 (Oct. 19, 1964), 45 cents.

Procedures for precise determination of thermal radiation properties November 1962 to October 1963, J. C. Richmond, D. P. DeWitt, and W. D. Hayes, Jr., NBS Tech. Note 252 (Nov. 20, 1964), 40 cents.

Publications In Other Journals

This column lists all publications by the NBS staff, as soon after issuance as practical. For completeness, earlier references not previously reported may be included from time to time.

Franck-Condon factors for the ionization of CO, NO, and O_2, M. E. Wacks, J. Chem. Phys. **41**, No. 4, 930–936 (Aug. 1964).

Versatile Stark waveguide for microwave spectroscopy, D. R. Lide, Jr., Rev. Sci. Instr. **35**, No. 9, 1226 (Sept. 1964).

Alkaline earth cation distributions in various borates, S. Block and G. J. Piermarini, Phys. and Chem. of Glasses **5**, No. 5, 138–144 (Oct. 1964).

Behavior of coaxial cable connectors for pulses with nanosecond risetimes, R. B. Schwartz and A. C. B. Richardson, Nuclear Instruments and Methods **29**, 83–88, North-Holland Publ. Co. (1964).

Theory of boil-off calorimetry, R. B. Jacobs, Rev. Sci. Instr. **35**, No. 7, 828–832 (July 1964).

"Thumbtack" accelerometer for the 1.5–150 kc range. P. Hertelendy and P. Reynard, Rev. Sci. Instr. **35**, No. 10, 1305–1306 (Oct. 1964).

Microwave spectroscopy, D. R. Lide, Jr., Ann. Rev. Phys. Chem. **15**, 225–250 (1964).

The application of Archimedes' principle to determination of the apparent volume of leather, J. R. Kanagy, J. Am. Leather Chem. Assoc. **LIX**, No. 11, 636–649 (Nov. 1964).

Growth spirals on $NiBr_2$ platelets, E. N. Sickafus and D. R. Winder, J. Appl. Phys. **35**, No. 8, 2541–2545 (Aug. 1964).

On the twilight sodium emission—1: Observations from a southern hemisphere station, M. Gadsden, Ann. Geophys. **20**, No. 3, 261–272 (1964).

Infrared spectrum of CF_3, D. E. Milligan, D. E. Mann, and M. E. Jacox, J. Chem. Phys. **41**, No. 5, 1199–1203 (Sept. 1, 1964).

Spectra tristimulus values for the CIE (u, v, w) uniform spacing system, I. Nimeroff, J. Opt. Soc. Am. (Letter to Editor) **54**, No. 11, 1365–1367 (Nov. 1964).

Proton-transfer reactions between H_3^+ and saturated hydrocarbons, P. Ausloos and S. G. Lias, J. Chem. Phys. **40**, No. 12, 3599–3605 (June 15, 1964).

Change in the heat capacity of boron trioxide during the glass transformation, S. S. Chang and A. B. Bestul, J. Phys. Chem. **68**, 3082 (1964).

Resinography with 8-Å X-rays, S. B. Newman, Symp. on Resinographic Methods, Special Tech. Publ. No. 348, ASTM (1963).

Microwave spectrum of the SO radical, F. X. Powell and D. R. Lide, Jr., J. Chem. Phys. **41**, No. 5, 1413–1419 (Sept. 1964).

Resonances of a spherical void in a compressible isotropic plasma, J. R. Wait, J. Geophys. Res. **69**, No. 19, 4189–4191 (Oct. 1, 1964).

The structure of the triclinic form of sodium tetramethaphosphate tetrahydrate, H. M. Ondik, Acta Cryst. **17**, No. 9, 1139–1145 (Sept. 1964).

Standards of electromotive force, W. J. Hamer, J. Wash. Acad. Sci. **54**, 297–315 (1964).

Experimental transition probabilities for six oxygen multiplets, J. E. Solarski and W. L. Wiese, Phys. Rev. **135**, No. 5A, A1236–A1241 (Aug. 31, 1964).

Electrochemical calorimetry III. Thermal effects of nickel-cadmium batteries, W. H. Metzger, Jr., and J. M. Sherfey, Electrochem. Technology **2**, No. 9–10, 285–289 (Sept.–Oct. 1964).

Evaluating computer systems analysis and design work in the Federal Government, W. H. Gammon, Book, Ideas for Management, Systems and Procedures 1964, 319–322 (1964).

Some remarks on microgrammars, W. C. Watt, Proc. Wash. Linguistics Club **2**, No. 1, 13–17 (Oct. 26, 1964).

Electrochemical calorimetry. IV. Measurement of the Peltier heat and voltage attending the passage of current across a liquid junction, A. Brenner and S. L. Gray, J. Electrochem. Soc. **111**, No. 11, 1225–1230 (Nov. 1964).

The National Bureau of Standards tritiated water standards, W. B. Mann, J. Appl. Rad. and Isotopes **15**, 628, Pergamon Press Ltd. (1964).

Microwave and high-frequency calibration services of the National Bureau of Standards, W. E. Larson, IEEE Trans. Microwave Theory Tech. **MTT–12**, No. 4, 480–482, (July 1964).

Diffusion in a polymer with lamellar morphology, polyethylene, R. K. Eby, J. Appl. Phys. **35**, No. 9, 2720–2724 (Sept. 1964).

Determination of the propagation constants for utrasonic waves in melting and molten polyethylene, R. K. Eby, J. Acoust. Soc. Am. **36**, No. 8, 1485–1487 (Aug. 1964).

Radiation from sources immersed in compressible plasma media, J. R. Wait, Can. J. Phys. **42**, 1760–1780 (Sept. 1964).

Conductance of copper m-benedisulfonate hexahydrate in N-methylpropionamide from 20 to 40°, T. B. Hoover, J. Phys. Chem. **68**, No. 10, 3003–3008 (Oct. 1964).

Polarized electrons and positrons by tagging technique, H. Olsen and L. C. Maximon, Phys. Rev. Letters **13**, No. 3, 112–114 (July 20, 1964).

Theory of whisker growth and evaporation, J. A. Simmons, R. L. Parker, and R. E. Howard, J. Appl. Phys. **35**, No. 7, 2271–2272 (July 1964).

Mass spectrometric study of the production of methylamine from azomethane, M. E. Wacks, J. Phys. Chem. **68**, No. 9, 2725–2726 (Sept. 1964).

Lasers for length measurement, A. G. McNish, Science **146**, No. 3641, 177–182 (Oct. 1964).

Infrared spectrum and structure of gaseous Al_2O, M. J. Linevsky, D. White, and D. E. Mann, J. Chem. Phys. **41**, No. 2, 542–545 (July 15, 1964).

High resolution infrared spectra $C_2{}^{12}H_2$, $C^{12}C^{13}H_2$, and $C_2{}^{13}H_2$, W. J. Lafferty and R. J. Thibault, J. Mol. Spectry. **14**, No. 1, 79–96 (Sept. 1964).

Gaussian correlation functions: Two-electron systems, W. A. Lester, Jr., J. Chem. Phys. **41**, No. 5, 1407–1413 (Sept. 1, 1964).

Nonspattering solder flux, W. R. Bjorklund, Rev. Sci. Instr. **35**, No. 10, 1369–1370 (Oct. 1964).

Use of the index of refraction as a means for study of plasma configurations, E. G. Johnson, Phys. Fluids **7**, 1551–1552 (Sept. 1964).

Application of the theory of absorbing Markov chains to the statistical thermodynamics of polymer chains in a lattice, J. Mazur, J. Chem. Phys. **41**, No. 8, 2256–2266 (Oct. 15, 1964).

A combinatorial problem and a simple decoding method for cyclic codes, M. Nesenbergs, IEEE Trans. Inform. Theory **IT–10**, 250–252 (July 1964).

Observed line shapes of collective excitations in Al, Be, and Ge, N. Swanson, J. Opt. Soc. Am. **54**, No. 9, 1130–1133 (Sept. 1964).

Flash-photolysis spectroscopy of matrices, L. J. Schoen and D. E. Mann, J. Chem. Phys. **41**, No. 5, 1514 (Sept. 1964).

Rotation-vibration interaction and other corrections to the spin doublet spearation in $^2\Pi$ diatomic molecules, T. C. James, J. Chem. Phys. **41**, No. 3, 631–641 (Aug. 1, 1964).

Publications for which a price is indicated are available by purchase from the Superintendent of Documents, U.S. Government Printing Office, Washington, D.C., 20402 (foreign postage, one-fourth additional). Reprints from outside journals and the NBS Journal of Research may often be obtained directly from the authors.

VOID

W. A.
ept. 1,

r. 35,

lasma
—1552

to the
attice,
ct. 15,

od for
Theory

d Ge,
(Sept.

n and
4).
e spin
ames,